Calculation of the Huang–Rhys parameter in spherical quantum dots: the optical deformation potential effect



2007 J. Phys.: Condens. Matter 19 346215

(http://iopscience.iop.org/0953-8984/19/34/346215)

IOP PUBLISHING JOURNAL OF PHYSICS: CONDENSED MATTER

J. Phys.: Condens. Matter **19** (2007) 346215 (12pp) doi:10.1088/0953-8984/19/34/346215

# Calculation of the Huang–Rhys parameter in spherical quantum dots: the optical deformation potential effect

**M Hamma**[1,2], **R P Miranda**[1,3], **M I Vasilevskiy**[1] **and I Zorkani**[2]

[1] Centro de Física, Universidade do Minho, 4170-057 Braga, Portugal
[2] LPS, Faculté des Sciences Dhar Mehraz, BP 1796, Fès, Morocco

Received 20 April 2007, in final form 30 May 2007
Published 24 July 2007
Online at stacks.iop.org/JPhysCM/19/346215

**Abstract**

An accurate calculation of the exciton–phonon interaction matrix elements and Huang–Rhys parameter for nearly spherical nanocrystals (NCs) of polar semiconductor materials is presented. The theoretical approach is based on a continuum lattice dynamics model and the effective mass approximation for electronic states in the NCs. A strong confinement regime is considered for both excitons and optical phonons, taking into account both the Fröhlich-type and optical deformation potential (ODP) mechanisms of the exciton–phonon interaction. The effects of exchange electron–hole interaction and possible hexagonal crystal structure of the underlying material are also taken into account. The theory is applied to CdSe and InP quantum dots. It is shown that the ODP mechanism, almost unimportant for CdSe, dominates the exciton–phonon coupling in small InP dots. The effect of the non-diagonal interaction, not included in the Huang–Rhys parameter, is briefly discussed.

(Some figures in this article are in colour only in the electronic version)

## 1. Introduction

During the last decade, intensive efforts have been devoted to studies of quasi-zero-dimensional semiconductor nanocrystals (NCs) possessing the properties of quantum dots (QDs). Technological improvements have been accompanied by theoretical work aiming at elucidating the QDs' properties. The electronic and optical properties of QDs are strongly influenced by optical phonons. In particular, the interaction of electrons and holes with optical phonons is important for steady-state and time-resolved optical absorption and emission spectra and inelastic light scattering by QDs. In recent years, it has become clear that the electron–phonon interaction in QDs leads to the formation of a polaron and cannot be described within the Born approximation [1–3]. A quantitative study of this interaction is crucial for achieving a

[3] Present address: Department of Physics and Astronomy, University College London, Gower Street, London WC1E 6BT, UK.

  

detailed understanding of the polaron properties in systems with discrete electron and exciton spectra. Therefore, it is important to use appropriate models for all polaron ingredients, i.e. electrons, holes and phonons.

There exists a broad literature devoted to the electronic structure of the most studied II–VI, III–V and elemental NCs (see e.g. [4]). Theoretical models that have been successfully applied to describe the electron and hole spectra of nearly spherical QDs range from the effective mass approximation (EMA) [5–7] to large scale *ab initio* calculations [8, 9]. There is a consensus that, if the complex valence band structure of the underlying material and the electron–hole exchange interaction are taken into account, the (semi-)analytical EMA calculations reproduce reasonably well the energy spectra and optical properties of confined excitons unless the QDs are too small (below 1 nm in radius).

The spatial confinement effect on optical phonons in semiconductor QDs has also been studied experimentally and theoretically (see [10] for a review). Again, continuum models provide a good understanding of experimental results obtained by means of Raman and far-infrared (FIR) spectroscopies [11, 12]. However, the intensity of the exciton–phonon interaction in QDs remains a controversial subject. Various theoretical studies led to different conclusions concerning the strength of the exciton–phonon interaction and its dependence on the QD size [13–16]. Klein *et al* [13] considered a donor-like exciton model (with a hole located at the centre of the dot) and the dielectric continuum model for phonons in a spherical QD. It was found that the Huang–Rhys parameter (HRP), a measure of the diagonal (or intra-level) exciton–phonon coupling, does not depend on the QD radius ($R$). On the other hand, Marini *et al* [14], who used a variational approach to determine the exciton ground-state wavefunction and a similar model for phonons, concluded that the HRP decreases with the increase of QD size in the strong confinement regime and changes little when $R$ becomes larger then the exciton Bohr radius, $a_{\mathrm{ex}}$. In contrast, calculations presented in [15, 16] predicted a strong size dependence of the exciton–phonon coupling strength in a spherical QD in the weak confinement regime.

From the experimental viewpoint, the exciton–phonon coupling strength was extracted from studies of Raman scattering by CuBr and CuCl QDs [17]. It was reported that the HRP increases monotonically with the decrease of the dot radius, for example, from 0.22 to 0.7 for CuCl QDs when $R$ decreased from 3 to 1.6 nm. Scamarcio *et al* [18] studied the size dependence of resonant Raman scattering by $CdS_xSe_{1-x}$ NCs embedded in a glass slab and reported an increase in the Fröhlich electron–phonon interaction strength with decreasing NC size within the strong confinement regime. Jungnickel *et al* [19] studied the luminescence from CdSe NCs in the situation of strong electron and hole confinement. They found that the HRP increases when the QD size is reduced, reaching a very high value of the order of unity for CdSe NCs with $R/a_{\mathrm{ex}} \approx 0.3$ [19].

This controversy, leading to the situation in which the exciton–phonon coupling constants are often treated as fitting parameters [3, 20], motivated the present work. We calculate the size dependence of the diagonal interaction between the ground-state exciton and optical phonons in a spherical QD by properly taking into account the confinement effect on the electron, hole and phonons, and including both the Fröhlich-type and optical deformation potential (ODP) mechanisms. The effects of phonon confinement and the dispersion of phonons with both electrostatic and mechanical boundary conditions have been considered in previous works [12, 21, 22] resulting in a good agreement with experimental data on Raman scattering in NCs of highly ionic materials such as CdSe. However, to the best of our knowledge, this is the first calculation of the ODP matrix elements for spherical QDs. The contribution of this mechanism is shown to be even more important than the Fröhlich-type one in the case of small InP dots. The effects of the electron–hole exchange interaction and hexagonal structure of the

underlying material on the HRP are also considered, leading to a reduction of its value for some states.

## 2. Exciton–phonon interaction Hamiltonian

In all semiconductors, excitons[4] interact with optical phonons by means of the deformation potential mechanism. In bulk semiconductors with cubic structure, for long-wavelength optical phonons, the ODP interaction vanishes by symmetry for any non-degenerate band (e.g. the $\Gamma_2$ conduction band in Ge or the $\Gamma_6$ conduction band in materials with zinc blende structure) [23] but it is non-zero for holes near the top of the valence band. The short-range ODP interaction is proportional to the relative displacement of two atoms in the same unit cell, with the corresponding operator given by [24]

$$\hat{H}'_{\mathrm{exL}} = \frac{\sqrt{3}d_0}{2a_0} \sum_{\nu} \vec{D} \cdot \vec{u}_{\nu}(\vec{r}), \tag{1}$$

where $a_0$ is the lattice constant and $d_0$ is the ODP constant for the $\Gamma^{v}_{15}$ valence band [23] and $\vec{u}_{\nu}$ is the relative displacement of two ions in the same unit cell for a phonon mode $\nu$. Considering only the light and heavy hole sub-bands ($\Gamma_8$), the vector $\vec{D}$ in equation (1) is constituted by numerical $4 \times 4$ matrices, $(D_x, D_y, D_z)$, with columns and rows corresponding to the Bloch states with different angular momentum projection $J_z = \pm 1/2, \pm 3/2$. The explicit form of these matrices can be found, for example, in [25].

In addition to $\hat{H}'_{\mathrm{exL}}$, the long-range electrostatic field associated with the optical vibrations in polar materials introduces a stronger coupling mechanism, the Fröhlich interaction. This interaction is described by the operator

$$\hat{H}''_{\mathrm{exL}} = e \sum_{\nu} \left[\varphi_{\nu}(\vec{r}_{\mathrm{h}}) - \varphi_{\nu}(\vec{r}_{\mathrm{e}})\right], \tag{2}$$

where $\vec{r}_{\mathrm{e}}(\vec{r}_{\mathrm{h}})$ is the electron (hole) radius-vector and $\varphi_{\nu}$ is the electrostatic potential associated with a confined phonon mode $\nu$.

Considering a spherical QD (of radius $R$) made of a material with isotropic phonon dispersion curves, confined phonon modes (which, in general, are mixed of longitudinal, transverse, and surface components) can be characterized by three 'spherical' quantum numbers, $\nu = \{l_p, m_p, n_p\}$. Using the formalism described in [11, 26, 27] for the case of perfect phonon confinement, the spherical components of the displacement vector are given by

$$\begin{aligned}
u^{r}_{l_p m_p n_p}(\vec{r}) &= \left(\frac{\hbar}{2\rho\omega_{l_p n_p}}\right)^{1/2} A_{l_p n_p} v_{l_p n_p}(r)\, Y_{l_p m_p}(\vartheta, \phi), \\
u^{\vartheta}_{l_p m_p n_p}(\vec{r}) &= \left(\frac{\hbar}{2\rho\omega_{l_p n_p}}\right)^{1/2} A_{l_p n_p} w_{l_p n_p}(r) \frac{\partial}{\partial\vartheta} Y_{l_p m_p}(\vartheta, \phi), \\
u^{\phi}_{l_p m_p n_p}(\vec{r}) &= \left(\frac{\hbar}{2\rho\omega_{l_p n_p}}\right)^{1/2} A_{l_p n_p} w_{l_p n_p}(r) \frac{1}{\sin\vartheta} \frac{\partial}{\partial\phi} Y_{l_p m_p}(\vartheta, \phi),
\end{aligned} \tag{3}$$

where $\rho$ is the reduced mass density, $\omega_{l_p n_p}$ denotes the eigenmode frequencies that are independent of $m_p$ and determined by a secular equation that can be found in [10, 11, 26]:

$$v_{l_p n_p}(r) = q_{l_p n_p} R j'_{l_p}(q_{l_p n_p} r) + \zeta_{l_p n_p} l_p (r/R)^{l_p - 1} + \frac{\eta_{l_p n_p} l_p (l_p + 1) R}{r} g_{l_p}(k_{l_p n_p} r),$$

$$w_{l_p n_p}(r) = \frac{R}{r}\left\{ j_{l_p}(q_{l_p n_p} r) + \zeta_{l_p n_p} (r/R)^{l_p} + \eta_{l_p n_p}\left[ g_{l_p}(k_{l_p n_p} r) + k_{l_p n_p} r g'_{l_p}(k_{l_p n_p} r)\right]\right\},$$

[4] By exciton we understand an electron–hole pair, independently of the confinement regime considered.

$$\zeta_{l_p n_p} = \{q_{l_p n_p} R j'_{l_p}(q_{l_p n_p} R)[g_{l_p}(k_{l_p n_p} R) + k_{l_p n_p} R g'_{l_p}(k_{l_p n_p} R) - l_p(l_p+1) j_{l_p}(q_{l_p n_p} R) g_{l_p}(k_{l_p n_p} R)]\} \times \{l_p[l_p g_{l_p}(k_{l_p n_p} R) - k_{l_p n_p} R g'_{l_p}(k_{l_p n_p} R)]\}^{-1},$$

$$\eta_{l_p n_p} = \frac{l_p j_{l_p}(q_{l_p n_p} R) - q_{l_p n_p} R\, j'_{l_p}(q_{l_p n_p} R)}{l_p[l_p g_{l_p}(k_{l_p n_p} R) - k_{l_p n_p} R\, g'_{l_p}(k_{l_p n_p} R)]},$$

$$q_{l_p n_p} = \sqrt{(\omega_{\mathrm{LO}}^2 - \omega_{l_p n_p}^2)/\beta_L}; \qquad k_{l_p n_p} = \sqrt{|(\omega_{\mathrm{TO}}^2 - \omega_{l_p n_p}^2)\beta_T|},$$

$Y_{l_p m_p}(\vartheta, \phi)$ is spherical harmonic, $j_{l_p}(x)$ a spherical Bessel function, $g_{l_p}(x)$ is equal to either $j_{l_p}(x)$ or $i^{-l_p} j_{l_p}(ix)$, depending on the sign of $(\omega_{\mathrm{TO}}^2 - \omega_{l_p n_p}^2)/\beta_T$; $\omega_{\mathrm{LO}}$, $\beta_L$ and $\omega_{\mathrm{TO}}$, $\beta_T$ are the bulk longitudinal optical (LO) and transverse optical (TO) phonon frequencies and bending parameters, respectively, and the normalization constant is determined by

$$A_{l_p n_p} = \left\{ \int_0^R [v_{l_p n_p}^2(r) + l_p(l_p+1) w_{l_p n_p}^2(r)]\, r^2\, \mathrm{d}r \right\}^{-1/2}.$$

The electrostatic potential is given by [27]

$$\varphi_{l_p m_p n_p}(\vec{r}) = \frac{C_{\mathrm{F}}}{e} \Phi_{l_p n_p}(r) Y_{l_p m_p}(\vartheta, \phi), \tag{4}$$

where $C_{\mathrm{F}} = e\sqrt{2\pi\hbar\omega_{\mathrm{LO}}(\varepsilon_\infty^{-1} - \varepsilon_0^{-1})/R}$ is the Fröhlich constant, with $\varepsilon_\infty$ and $\varepsilon_0$ being the high-frequency and static dielectric constants of the QD material, respectively. The dimensionless function $\Phi$ in equation (4) is

$$\Phi_{l_p n_p}(r) = A_{l_p n_p}\left[ j_{l_p}(q_{l_p n_p} r) + \gamma_{l_p n_p} \zeta_{l_p n_p} (r/R)^{l_p} \right],$$

where $\gamma_{l_p n_p} = (\omega_{l_p n_p}^2 - \omega_{\mathrm{TO}}^2)/(\omega_{\mathrm{LO}}^2 - \omega_{\mathrm{TO}}^2)$. Note that the above expressions are valid for $l_p > 0$. Expressions for $l_p = 0$ can be found, for example, in [10, 22, 28].

## 3. Exciton ground state and matrix elements

Within the EMA, a relatively simple description of electron–hole pair states confined in a spherical QD is possible in the limiting case of strong exciton confinement ($R \ll a_{\mathrm{ex}}$). In the first approximation, the exciton wavefunction can be factorized:

$$\Psi_{\mathrm{ex}}(\vec{r}_{\mathrm{e}}, \vec{r}_{\mathrm{h}}) = \Psi_{\mathrm{h}}(\vec{r}_{\mathrm{h}}) \Psi_{\mathrm{e}}(\vec{r}_{\mathrm{e}}). \tag{5}$$

The lowest-energy state for electrons belonging to the $\Gamma_6$ conduction band is two-fold degenerate due to the spin projection $s_z = \pm 1/2$, with the wavefunctions given by $\Psi_{\mathrm{e}}^{s_z}(\vec{r}) = \psi_0(\vec{r})\delta_{s_z,\sigma}|\sigma\rangle$, where $|\sigma\rangle$ is the Bloch function of the $\Gamma_6$ band, labelled by $\sigma = \uparrow, \downarrow$. The envelope function can be found in many books and papers (e.g. [4–6]):

$$\psi_0(\vec{r}) = \theta(R - r)\sqrt{\frac{2\pi^2}{R^3}}\, j_0(\pi r/R) Y_{00}(\vartheta, \phi), \tag{6}$$

where $\theta(R - r)$ is the Heaviside function. For the four-fold degenerate hole ground state[5] with total angular momentum $F_{\mathrm{h}} = 3/2$, usually denoted by $1\mathrm{S}_{3/2}$, the wavefunctions are written as [5, 6]

$$\Psi_{\mathrm{h}}^M(\vec{r}) = 2 \sum_{l=0,2} R_l(r)(-1)^{M-\frac{3}{2}} \sum_{\mu+m=M} \begin{pmatrix} 3/2 & l & 3/2 \\ \mu & m & -M \end{pmatrix} Y_{lm}(\vartheta, \phi)|\mu\rangle, \tag{7}$$

[5] We consider the case of large spin–orbit interaction neglecting the $\Gamma_7$ band.

where $M = \pm 1/2, \pm 3/2, |\mu\rangle$ are the Bloch functions of the $\Gamma_8$ band ($\mu = \pm 1/2, \pm 3/2$) and $\begin{pmatrix} \cdots \\ \cdots \end{pmatrix}$ are the Wigner 3-$j$ symbols. The radial envelope functions are given by

$$\begin{aligned} R_0(r) &= \theta(R-r)\frac{C}{R^{3/2}}\left[j_0(K_{\mathrm{h}}r) - \frac{j_0(K_{\mathrm{h}}R)}{j_0(\sqrt{\beta}K_{\mathrm{h}}R)}j_0(\sqrt{\beta}K_{\mathrm{h}}r)\right], \\ R_2(r) &= \theta(R-r)\frac{C}{R^{3/2}}\left[j_2(K_{\mathrm{h}}r) + \frac{j_0(K_{\mathrm{h}}R)}{j_0(\sqrt{\beta}K_{\mathrm{h}}R)}j_2(\sqrt{\beta}K_{\mathrm{h}}r)\right], \end{aligned} \tag{8}$$

where $C$ is a normalization constant, $\beta = m_{\mathrm{lh}}/m_{\mathrm{hh}}$ is the ratio of the light and heavy hole masses, and $K_{\mathrm{h}} = \chi_1/R$ with $\chi_1$ denoting the first root of a certain characteristic equation [5, 6].

Calculation of the matrix elements of the Fröhlich-type part of the exciton–phonon interaction Hamiltonian (2) using expressions (4)–(8) is straightforward. They are non-zero only for phonons with $l_p = 0, 2$. The result is expressed in terms of two integrals,

$$J_{0n_p} = \frac{C_{\mathrm{F}}}{\sqrt{4\pi}}\int_0^R [R_0^2(r) + R_2^2(r) - \psi_0^2(r)]\Phi_{0n_p}(r)r^2\,\mathrm{d}r \tag{9}$$

and

$$J_{2n_p} = \frac{C_{\mathrm{F}}}{\sqrt{5\pi}}\int_0^R R_0(r)R_2(r)\Phi_{2n_p}(r)r^2\,\mathrm{d}r. \tag{10}$$

All the diagonal matrix elements are equal to $J_{0n_p}$ for $l_p = 0$, while for $l_p = 2, m_p = 0$ they are equal to $\pm J_{2n_p}$, depending on the sign of $M$.

Calculation of the ODP matrix elements is more tedious and, to the best of our knowledge, has not been performed before. We express the scalar product in (1) in terms of spherical components of the displacement,

$$\begin{aligned} \vec{D}\cdot\vec{u}_{l_pm_pn_p} &= (D_x\sin\vartheta\cos\phi + D_y\sin\vartheta\sin\phi + D_z\cos\vartheta)u^r_{l_pm_pn_p} \\ &\quad + (D_x\cos\vartheta\cos\phi + D_y\cos\vartheta\sin\phi - D_z\sin\vartheta)u^{\vartheta}_{l_pm_pn_p} \\ &\quad + (-D_x\sin\phi + D_y\cos\phi)u^{\phi}_{l_pm_pn_p}, \end{aligned}$$

and expand the three terms in series of spherical harmonics,

$$\vec{D}\cdot\vec{u}_{l_pm_pn_p} = \vec{D}\cdot\sum_{L,M}(\vec{A}^{l_pm_pn_p}_{\mathrm{LM}} + \vec{B}^{l_pm_pn_p}_{\mathrm{LM}} + \vec{C}^{l_pm_pn_p}_{\mathrm{LM}})Y_{\mathrm{LM}}(\theta,\phi), \tag{11}$$

with $\vec{A}^{l_pm_pn_p}_{\mathrm{LM}} = (a^{l_pm_pn_p;x}_{\mathrm{LM}}; a^{l_pm_pn_p;y}_{\mathrm{LM}}; a^{l_pm_pn_p;z}_{\mathrm{LM}})$ and similarly for $\vec{B}^{l_pm_pn_p}_{\mathrm{LM}}$ and $\vec{C}^{l_pm_pn_p}_{\mathrm{LM}}$. For example,

$$a^{l_pm_pn_p;x}_{\mathrm{LM}} = \left(\frac{\hbar}{2\rho\omega_{l_pn_p}}\right)^{1/2}A_{l_pn_p}v_{l_pn_p}(r)\cdot\int\cos\vartheta\,Y^*_{\mathrm{LM}}(\theta,\phi)Y_{l_pm_p}(\theta,\phi)\,\mathrm{d}\Omega.$$

After finding the expansion coefficients in (11), we can calculate the ODP matrix elements, which are non-zero only for phonons with $l_p = 1, 3$. Note that only holes are involved in this interaction. For $l_p = 1, m_p = 0$, the diagonal matrix elements are equal to $C_{1n_p}I^-_{10n_p}$ for $M = \pm 3/2$ and to $C_{1n_p}I^+_{10n_p}$ for $M = \pm 1/2$, with

$$I^{\pm}_{10n_p} = \frac{2d_0}{5\sqrt{3\pi}}\int_0^R\left(R_0(r)R_2(r) \pm \frac{1}{7}R_2^2(r)\right)\left[v_{l_pn_p}(r) - w_{l_pn_p}(r)\right]r^2\,\mathrm{d}r. \tag{12}$$

For phonons with $l_p = 3$, the non-zero contributions arise from the modes with $m_p = 0$ and from those with $m_p = \pm 2$. In the former case, the diagonal matrix elements are equal to $C_{3n_p}I^-_{30n_p}$ for $M = \pm 3/2$ and to $C_{3n_p}I^+_{30n_p}$ for $M = \pm 1/2$, with

$$I^{\pm}_{30n_p} = \frac{2d_0}{5\sqrt{7\pi}}\int_0^R\left(R_0(r)R_2(r) \pm \frac{1}{7}R_2^2(r)\right)\left[v_{l_pn_p}(r) + 4w_{l_pn_p}(r)\right]r^2\,\mathrm{d}r. \tag{13}$$

In the latter case, they are equal to $\mathrm{i}\frac{m_p}{|m_p|}C_{3n_p}I^{+}_{32n_p}$ for $M=\pm 3/2$ and to $\mathrm{i}\frac{m_p}{|m_p|}C_{3n_p}I^{-}_{32n_p}$ for $M=\pm 1/2$, where

$$I^{\pm}_{32n_p}=\frac{d_0}{\sqrt{210\pi}}\int_0^R\left(R_0(r)R_2(r)\pm\frac{2}{7}R_2^2(r)\right)\left[v_{l_pn_p}(r)+4w_{l_pn_p}(r)\right]r^2\,\mathrm{d}r. \tag{14}$$

The dimensionless constants $C_{l_pn_p}$ in the above expressions are given by

$$C_{l_pn_p}=\frac{\sqrt{3}}{2a_0}\left(\frac{\hbar}{2\rho\omega_{l_pn_p}}\right)^{1/2}A_{l_pn_p}, \tag{15}$$

with corresponding $l_p$ and $n_p$.

## 4. Effects of exchange interaction and hexagonal crystal structure

As is known, the eight-fold degenerate exciton state $1\mathrm{s_e}1\mathrm{S}_{3/2}$ is split by the electron–hole exchange interaction and, additionally, by the crystal field if the underlying QD material has hexagonal structure. These effects were considered in detail in [5, 6]. The result is that there are five energy levels corresponding to the exciton states with different total angular momentum, denoted $0^{\mathrm{U}}$, $0^{\mathrm{L}}$, $\pm1^{\mathrm{U}}$, $\pm1^{\mathrm{L}}$ and $\pm2$. The energies of these states and the corresponding wavefunctions are determined by two parameters,

$$\eta=\frac{\varepsilon_{\mathrm{exch}}a_0^3}{3\pi R}\int_0^R\sin^2\left(\frac{\pi r}{R}\right)\left(R_0^2(r)+\frac{1}{5}R_2^2(r)\right)\mathrm{d}r \tag{16}$$

and

$$\Delta=\Delta_{\mathrm{cr}}\int_0^R\left(R_0^2(r)-\tfrac{3}{5}R_2^2(r)\right)r^2\,\mathrm{d}r, \tag{17}$$

where $\varepsilon_{\mathrm{exch}}$ and $\Delta_{\mathrm{cr}}$ are the exchange interaction and crystal-field constants of the corresponding bulk material.

We can obtain the exciton–phonon interaction parameters for the $0^{\mathrm{U}}$, $0^{\mathrm{L}}$, $\pm1^{\mathrm{U}}$, $\pm1^{\mathrm{L}}$ and $\pm2$ states from those calculated in the previous section by using the transformation matrix that relates these two bases. This matrix, with elements entirely determined by the parameters (16) and (17), has been presented in [22]. The result of the calculation is most conveniently presented in matrix form, with the lines and rows corresponding to the states $0^{\mathrm{U}}$, $0^{\mathrm{L}}$, $+1^{\mathrm{U}}$, $+1^{\mathrm{L}}$, $-1^{\mathrm{U}}$, $-1^{\mathrm{L}}$, $+2$, and $-2$ (in this order):

$$B^{(l_p,0,n_p)}=C_{l_pn_p}\times\begin{pmatrix} I^{+}_{l_p0n_p} & 0 & 0 & 0 & 0 & 0 & 0 & 0\\ 0 & I^{+}_{l_p0n_p} & 0 & 0 & 0 & 0 & 0 & 0\\ 0 & 0 & \tilde{I}^{-}_{l_p0n_p} & cI_{l_p0n_p} & 0 & 0 & 0 & 0\\ 0 & 0 & cI_{l_p0n_p} & \tilde{I}^{+}_{l_p0n_p} & 0 & 0 & 0 & 0\\ 0 & 0 & 0 & 0 & \tilde{I}^{-}_{l_p0n_p} & -cI_{l_p0n_p} & 0 & 0\\ 0 & 0 & 0 & 0 & -cI_{l_p0n_p} & \tilde{I}^{+}_{l_p0n_p} & 0 & 0\\ 0 & 0 & 0 & 0 & 0 & 0 & I^{-}_{l_p0n_p} & 0\\ 0 & 0 & 0 & 0 & 0 & 0 & 0 & I^{-}_{l_p0n_p} \end{pmatrix} \tag{18}$$

for the phonons with $l_p = 1, 3$ and $m_p = 0$, and

$$B^{(3,\pm 2,n_p)} = C_{3n_p} \times \begin{pmatrix} \pm \mathrm{i} I^-_{32n_p} & 0 & 0 & 0 & 0 & 0 & 0 & 0 \\ 0 & \pm \mathrm{i} I^-_{32n_p} & 0 & 0 & 0 & 0 & 0 & 0 \\ 0 & 0 & \pm \mathrm{i} \tilde{I}^+_{32n_p} & \pm \mathrm{i} c I_{32n_p} & 0 & 0 & 0 & 0 \\ 0 & 0 & \pm \mathrm{i} c I_{32n_p} & \pm \mathrm{i} \tilde{I}^-_{32n_p} & 0 & 0 & 0 & 0 \\ 0 & 0 & 0 & 0 & \pm \mathrm{i} \tilde{I}^+_{32n_p} & \mp \mathrm{i} c I_{32n_p} & 0 & 0 \\ 0 & 0 & 0 & 0 & \mp \mathrm{i} c I_{32n_p} & \pm \mathrm{i} \tilde{I}^-_{32n_p} & 0 & 0 \\ 0 & 0 & 0 & 0 & 0 & 0 & \pm \mathrm{i} I^+_{32n_p} & 0 \\ 0 & 0 & 0 & 0 & 0 & 0 & 0 & \pm \mathrm{i} I^+_{32n_p} \end{pmatrix} \tag{19}$$

for the phonons with $l_p = 3$ and $m_p = \pm 2$. In the expressions (18) and (19), $C_{l_p n_p}$ is given by equation (15):

$$\tilde{I}^{\pm}_{l_p m_p n_p} = (I^+_{l_p m_p n_p} + I^-_{l_p m_p n_p})/2 \pm b(I^+_{l_p m_p n_p} - I^-_{l_p m_p n_p})/2,$$

$$I_{l_p m_p n_p} = (I^+_{l_p m_p n_p} - I^-_{l_p m_p n_p})/2,$$

with $I^{\pm}_{l_p m_p n_p}$ given by equations (12)–(14):

$$b = \frac{2\eta - \Delta}{\sqrt{16\eta^2 + \Delta^2 - 4\eta\Delta}},$$

and

$$c = \frac{2\sqrt{3}\eta}{\sqrt{16\eta^2 + \Delta^2 - 4\eta\Delta}}.$$

For the sake of completeness, we reproduce here the exciton–phonon interaction matrix for the phonons with $l_p = 2$ and $m_p = 0$ (Fröhlich-type mechanism) [22]:

$$B^{(2,0,n_p)} = J_{2n_p} \begin{pmatrix} 1 & 0 & 0 & 0 & 0 & 0 & 0 & 0 \\ 0 & 1 & 0 & 0 & 0 & 0 & 0 & 0 \\ 0 & 0 & -b & c & 0 & 0 & 0 & 0 \\ 0 & 0 & c & b & 0 & 0 & 0 & 0 \\ 0 & 0 & 0 & 0 & -b & -c & 0 & 0 \\ 0 & 0 & 0 & 0 & -c & b & 0 & 0 \\ 0 & 0 & 0 & 0 & 0 & 0 & -1 & 0 \\ 0 & 0 & 0 & 0 & 0 & 0 & 0 & -1 \end{pmatrix}. \tag{20}$$

For the $l_p = 0$ phonons, the matrix remains diagonal with all non-zero elements equal to $J_{0n_p}$.

## 5. Calculated results for the HRP

First, we would like to recall that the Huang–Rhys parameter (HRP), $S$, is a dimensionless measure of the exciton–optical-phonon interaction. It can be defined with rigour in the framework of the so-called independent boson model (IBM) [29, 30] describing the coupling of a *single non-degenerate* exciton level to a gas of phonons at equilibrium. The picture changes when the exciton state is degenerate or there are several states separated by energies that are small compared to $\hbar\omega_{\mathrm{LO}}$. Various definitions of the HRP have been proposed but none of them is completely satisfactory [31], since the adiabatic approximation becomes insufficient [21].

Considering the HRP as a simple measure of the exciton–phonon interaction we define it for each sub-state $(s_z, M)$ constituting the $1s_e1S_{3/2}$ QD exciton octet, in the same way as for a non-degenerate state [30, 31]:

$$S_{s_z,M} = (\hbar\omega_{\mathrm{LO}})^{-2} \sum_{l_p,m_p,n_p} \left|\langle \Psi_{\mathrm{ex}}^{s_z,M} \left| H_{\mathrm{ex-ph}} \right| \Psi_{\mathrm{ex}}^{s_z,M} \rangle\right|^2 . \tag{21}$$

If the $(s_z, M)$ states were non-degenerate, this parameter would determine the downward shift of their energy (the so-called polaron correction),

$$\Delta E_{s_z,M} = \sum_{l_p,m_p,n_p} \frac{|\langle \Psi_{\mathrm{ex}}^{s_z,M} | H_{\mathrm{ex-ph}} | \Psi_{\mathrm{ex}}^{s_z,M} \rangle|^2}{\hbar\omega_{l_p m_p n_p}} \approx S_{s_z,M}\hbar\omega_{\mathrm{LO}}, \tag{22}$$

and also the relative intensity of the equidistant satellites of the main peak in the absorption and emission spectra if one takes $\omega_{l_p m_p n_p} \approx \omega_{\mathrm{LO}}$ for all phonon modes. In the real situation, the true polaron correction depends on both diagonal and non-diagonal matrix elements of the exciton–phonon interaction Hamiltonian. Nevertheless, we shall use the HRP defined by equation (21) as a meaningful single quantity characterizing the exciton–lattice coupling and allowing for the comparison of the relative importance of the two mechanisms considered in this work.

Let us first neglect the effects of exchange interaction and hexagonal crystal field. It turns out that, if only the Fröhlich-type interaction is taken into account, $S$ is exactly the same for all eight states, within the approximation considered. The ODP interaction introduces some difference between the states with $M = \pm 3/2$ and $\pm 1/2$. According to the HRP definition (21) and results presented in section 3,

$$S_{s_z,M} = (\hbar\omega_{\mathrm{LO}})^{-2} \sum_{n_p} \left\{ J_{0n_p}^2 + J_{2n_p}^2 + (C_{1n_p} I_{10n_p}^{\pm})^2 + (C_{3n_p} I_{30n_p}^{\pm})^2 + 2(C_{3n_p} I_{32n_p}^{\mp})^2 \right\}, \tag{23}$$

where the upper and lower sign applies to the states with $M = \pm 1/2$ and $\pm 3/2$, respectively. The radial dependence of the HRP calculated according to equation (23) is presented in figures 1 and 2 for CdSe and InP QDs, respectively. The material parameters used in the calculations are listed in table 1. As can be seen from figure 1, the difference between these two groups of states is fairly small in the case of CdSe dots where the Fröhlich-type interaction is dominant and the ODP contribution to the HRP does not exceed 10% (consequently, $S$ scales approximately as $R^{-1}$).

The case of InP QDs is different. This material is characterized by a lower degree of ionicity and a larger ODP interaction constant. As a result, the ODP and Fröhlich-type mechanisms produce comparable contributions to the HRP and the difference between the exciton states involving $M = \pm 1/2$ and $\pm 3/2$ holes becomes significant (see figure 2). There is no simple scaling law for $S$ versus $R$ in this case.

With the effects considered in section 4 taken into account, expression (23) holds for the states $0^{\mathrm{U}}$ and $0^{\mathrm{L}}$ (with the upper sign), and $\pm 2$ (with the lower sign), as can be seen from equations (18)–(20). At the same time, the HRP value for the remaining states is given by a different expression, namely,

$$S_{\pm 1^{\mathrm{U,L}}} = (\hbar\omega_{\mathrm{LO}})^{-2} \sum_{n_p} \left\{ J_{0n_p}^2 + b^2 J_{2n_p}^2 + (C_{1n_p} \tilde{I}_{10n_p}^{\pm})^2 + (C_{3n_p} \tilde{I}_{30n_p}^{\pm})^2 + 2(C_{3n_p} \tilde{I}_{32n_p}^{\mp})^2 \right\}. \tag{24}$$

In equation (24), the upper (lower) sign applies to the $\pm 1^{\mathrm{L}}$ ($\pm 1^{\mathrm{U}}$) states. The values of $S_{\pm 1^{\mathrm{U,L}}}$ versus QD radius are also presented in figures 1 and 2.

Among the material parameters used in these calculations, the ratio of the light and heavy hole masses ($\beta$) is probably less well known. Meanwhile, the values of the exciton–phonon interaction parameters depend strongly on $\beta$. Figures 3 and 4 show the HRP variation with $\beta$ for CdSe and InP QDs with $R = 2$ nm.

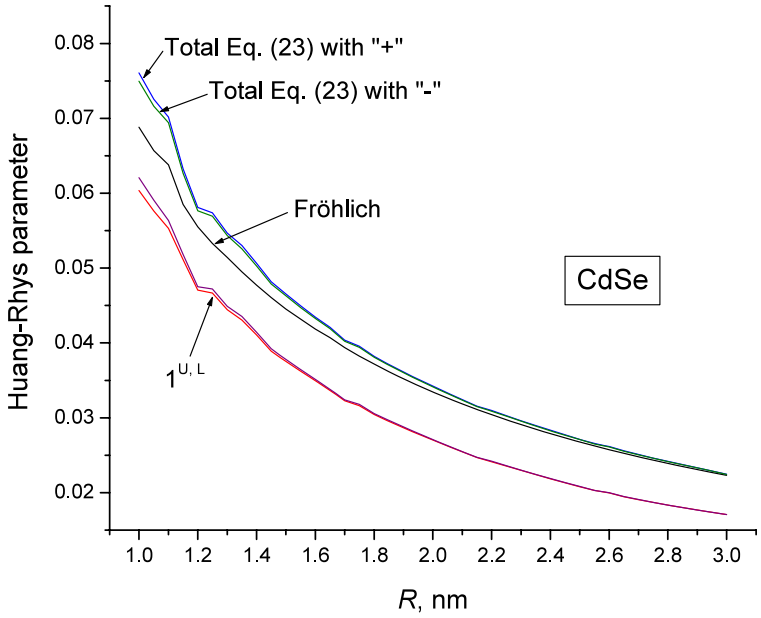


**Figure 1.** HRP calculated for CdSe QDs of different radii, with and without exchange interaction and crystal-field effects. In the latter case, $\pm$ corresponds to the $M = \pm 1/2$ and $\pm 3/2$ states, respectively. Also shown is the contribution of the Fröhlich-type mechanism. The curves labelled $1^{U,L}$ represent the exchange interaction and crystal-field effects that affect only these four states. $\beta = 0.16$ was used in these calculations.

**Table 1.** Material parameters used in the calculations.

| Parameters | CdSe | InP |
|---|---|---|
| $m_e/m_0$ | 0.13 | 0.08 |
| $m_{lh}/m_0$ | 0.26 | 0.09 |
| $\varepsilon_0$ | 9.7 | 12.5 |
| $\varepsilon_\infty$ | 6.2 | 9.7 |
| $\Delta_{cr}$ (meV) | 25 | 0 |
| $\varepsilon_{exch} a_0^3$ (meV nm$^3$) | 36 | 36 |
| $\omega_{LO}$ (cm$^{-1}$) | 211 | 348 |
| $\omega_{TO}$ (cm$^{-1}$) | 169 | 307 |
| $d_0$ (eV) | 8.9 | 35.6 |
| $a_0$ (A) | 6.05 | 5.87 |
| $\beta_{LO}$ (cm$^{-1}$ A$^2$) | 70.55 | 29.43 |
| $\beta_{TO}$ (cm$^{-1}$ A$^2$) | $-35.08$ | $-15.6$ |

## 6. Discussion and conclusion

We have calculated the Huang–Rhys parameter for the ground-state exciton strongly confined in a spherical QD using a self-consistent approach and taking into account both the Fröhlich-type and ODP mechanisms. We did not use any simplified (e.g. donor-like) model for the exciton as was the case of some previous calculations. Our treatment includes the light/heavy hole mixing, which is the major source of the electron and hole charge separation in a QD embedded in a dielectric matrix, thus contributing to the enhanced net exciton–phonon interaction via the Fröhlich-type mechanism. For the first time, the ODP contribution has been incorporated. The

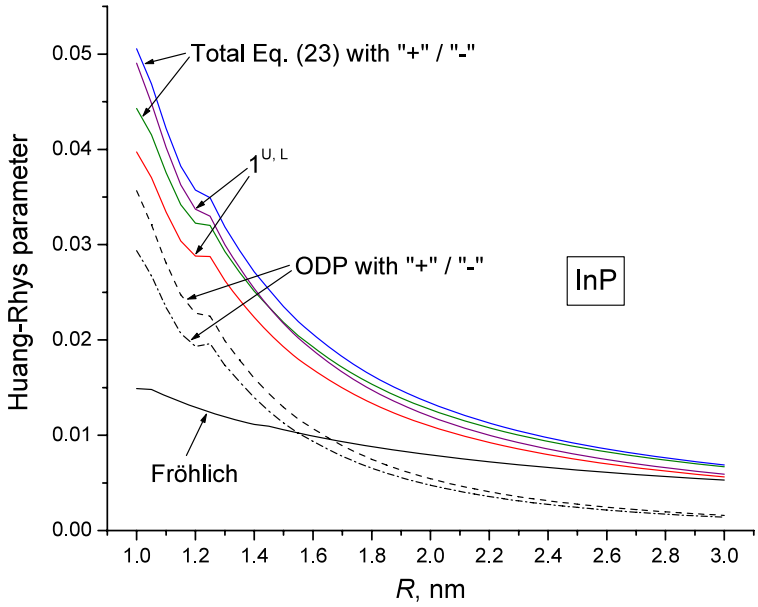


**Figure 2.** The same as in figure 1 but for InP QDs. Additionally, the ODP mechanism contribution is shown explicitly (calculated without exchange interaction effect). $\beta = 0.16$.

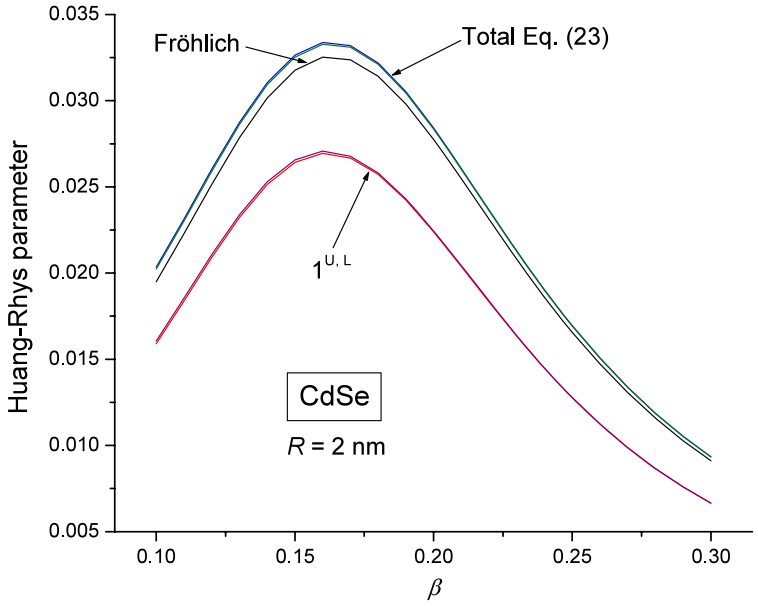


**Figure 3.** The same quantities as in figure 1 plotted against the light/heavy hole mass ratio. CdSe QD radius 2 nm.

results show that, for CdSe dots, the HRP can hardly exceed a moderate value of $S \approx 0.05$, within the limits of validity of the effective mass theory for electrons and holes, and continuous lattice dynamics model for phonons. This is at least an order of magnitude smaller than the so-called experimental values, usually derived from the ratio of the measured intensities of the

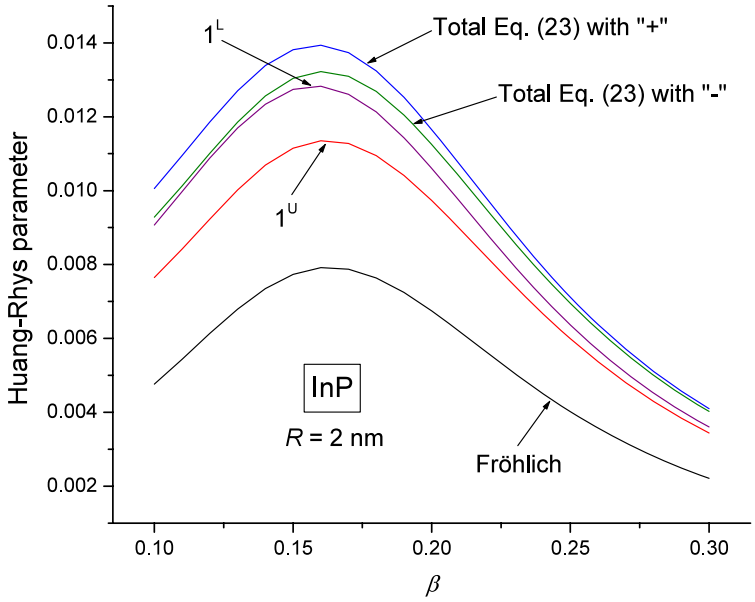


**Figure 4.** The same quantities as in figure 2 plotted against the light/heavy hole mass ratio. InP QD radius 2 nm.

phonon satellites in the QD emission spectra [19, 32, 33]. We believe that the present theory provides correct values of the exciton–phonon interaction parameters in spherical QDs. The apparent discrepancy with experiment is due to the fact that the adiabatic IBM is insufficient to describe the exciton–polaron spectra of QDs. This was first pointed out by the authors of [34], who noticed that, in some cases (e.g. [33]), no HRP value can allow one to fit the experimental spectra with the theory based on the adiabatic IBM [29, 30]. As a result of the phonon-induced mixing of exciton states, the energy spectrum of the QD can be drastically changed. Examples of this effect on the absorption, emission and Raman spectra of QDs can be found in [3, 21, 22].

However, in spite of the limited applicability of the adiabatic approximation, the HRP is still a meaningful parameter that mainly determines the polaron shift of the zero-phonon line according to equation (22). In spherical QDs, phonon-mediated coupling between different exciton states is expected to be weaker then the diagonal one because phonons with $l_p = 0$ do not contribute to the former[6]. Consequently, the fine structure of the spectra, originating from the phonon-induced mixing of different exciton states, may not be resolved in spectroscopic experiments even when a small number of QDs is probed [35] and the polaron shift (22) is supposed to be the major effect. The presented theory predicts different polaron shifts for different optically active states of the $1s_e1S_{3/2}$ octet. The difference can reach as much as $0.005\hbar\omega_{LO}$ (approximately corresponding to 1 $cm^{-1}$) for both CdSe and InP QDs. It should contribute to the homogeneous broadening of the emission line, decreasingly as the QD size increases.

In conclusion, we have performed calculations of the Huang–Rhys parameter for a spherical QD made of a polar semiconductor material and have presented illustrative results for CdSe and InP dots. The relevant exciton–phonon interaction matrix elements are non-zero

[6] As mentioned at the end of section 4, the interaction matrix for such modes is diagonal and reduces to a single coupling constant. Although its value is reduced because of the partial compensation of the electron and hole clouds in the QD, it is still quite considerable, compared to the other phonon modes.

for phonon modes with $l_p = 0, 2$ (Fröhlich-type mechanism) and $l_p = 1, 3$ (ODP mechanism). The results calculated for InP and CdSe are shown to be quite sensitive to the ratio of light and heavy hole masses. As the confinement becomes stronger, the HRP value increases rapidly, although, in general, there is no simple scaling law for it with the QD size. For CdSe, the Fröhlich-type mechanism is by far more important than the ODP. For InP, both mechanisms are important and, for $R \leqslant 2$ nm, the largest contribution comes from the $l_p = 3$ modes. We also considered the effect of the hexagonal crystal structure (for CdSe) and exchange interaction on the HRP and found that its value is different for $\pm 1^{\mathrm{U,L}}$, $0^{\mathrm{U,L}}$ and $\pm 2$ exciton states. This implies different polaron shifts for these groups of states.

## Acknowledgment

This work was supported by the FCT (Portugal) through project POCI/FIS/58524/2004.

## References

[1] Li X Q and Arakawa Y 1998 *Phys. Rev.* B **57** 12285
[2] Verzelen O, Ferreira R and Bastard G 2002 *Phys. Rev. Lett.* **88** 146803
[3] Vasilevskiy M I, Anda E V and Makler S S 2004 *Phys. Rev.* B **70** 35318
[4] Woggon U 1999 *Optical Properties of Semiconductor Quantum Dots* (Heidelberg: Springer)
[5] Efros Al L 1992 *Phys. Rev.* B **46** 7448
[6] Efros Al L, Rosen M, Kuno M, Nirmal M, Norris D J and Bawendi M 1996 *Phys. Rev.* B **54** 4843
[7] Prado S J, Trallero-Giner C, Alcalde A M, López-Richard V and Marques G E 2003 *Phys. Rev.* B **68** 235327
[8] Wang L-W and Zunger A 1996 *Phys. Rev.* B **53** 9579
[9] Delerue C and Lannoo M 2004 *Nanostructures. Theory and Modelling* (Berlin: Springer)
[10] Rolo A and Vasilevskiy M I 2007 *J. Raman Spectrosc.* **38** 618
[11] Vasilevskiy M I 2002 *Phys. Rev.* B **66** 195326
[12] Trallero-Giner C, Debernardi A, Cardona M, Menendez-Proupin E and Ekimov A I 1998 *Phys. Rev.* B **57** 4664
[13] Klein M C, Hache F, Ricard D and Flytzanis C 1990 *Phys. Rev.* B **42** 11123
[14] Marini J C, Stebe B and Kartheuser E 1994 *Phys. Rev.* B **50** 14302
[15] Fedorov A V and Baranov A V 1996 *Sov. Phys.—JETP* **83** 610
[16] Ajiki H 2001 *Phys. Status Solidi* b **224** 633
[17] Fedorov A V, Baranov A V and Inoue K 1997 *Phys. Rev.* B **56** 7491
Baranov A V, Yamaguchi S and Masumoto Y 1997 *Phys. Rev.* B **56** 10302
[18] Scamarcio G, Spagnolo V, Ventrruti G, Lugara M and Righini G C 1996 *Phys. Rev.* B **53** R10489
[19] Jungnickel V and Henneberger F 1996 *J. Lumin.* **70** 238
[20] Stauber T, Zimmermann R and Castella H 2000 *Phys. Rev.* B **62** 7336
[21] Pokatilov E P, Klimin S N, Fomin V M, Gladilin V N, Devreese J T and Wise F W 1998 *Phys. Rev.* B **65** 075316
[22] Miranda R P, Vasilevskiy M I and Trallero-Ginner C 2006 *Phys. Rev.* B **74** 115317
[23] Blacha A, Presting H and Cardona M 1984 *Phys. Status Solidi* b **126** 11
[24] Woerner M and Elsaesser T 1995 *Phys. Rev.* B **51** 17490
[25] Dargys A 2005 *Semicond. Sci. Technol.* **20** 733
[26] Roca E, Trallero-Ginner C and Cardona M 1994 *Phys. Rev.* B **49** 13704
[27] Chamberlain M P, Trallero-Ginner C and Cardona M 1995 *Phys. Rev.* B **51** 1680
[28] Vasilevskiy M I, Rolo A G, Gomes M J M, Vikhrova O V and Ricolleau C 2001 *J. Phys.: Condens. Matter* **13** 3491
[29] Mahan G D 2000 *Many-Particle Physics* (New York: Kluwer–Academic)
[30] Schmitt-Rink S, Miller D A B and Chemla S 1987 *Phys. Rev.* B **35** 8113
[31] Stoneham A M 1996 *Theory of Defects in Solids* (Oxford: Clarendon) chapter 10
[32] Bissiri M, von Högersthal G B, Bhatti A S, Capizzi M, Frova A, Frigeri P and Franchi S 2000 *Phys. Rev.* B **62** 4642
[33] Nirmal M, Murray C B, Norris D J and Bawendi M G 1993 *Z. Phys.* D **26** 361
[34] Fomin V M, Gladilin V N, Devreese J T, Pokatilov E P, Balaban S N and Klimin S N 1998 *Phys. Rev.* B **57** 2415
[35] Empedocles S A, Norris D J and Bawendi M G 1996 *Phys. Rev. Lett.* **77** 3873